MISSOURI S&T

Missouri University of Science and Technology
Scholars' Mine

International Conferences on Recent Advances in Geotechnical Earthquake Engineering and Soil Dynamics

1991 - Second International Conference on Recent Advances in Geotechnical Earthquake Engineering & Soil Dynamics

Mar 11th - Mar 15th

A Cyclic Shear-Volume Coupling and Pore Pressure Model for Sand

Peter M. Byrne
University of British Columbia, Vancouver, B.C., Canada

Follow this and additional works at: http://scholarsmine.mst.edu/icrageesd

 Part of the Geotechnical Engineering Commons

Recommended Citation

Byrne, Peter M., "A Cyclic Shear-Volume Coupling and Pore Pressure Model for Sand" (1991). *International Conferences on Recent Advances in Geotechnical Earthquake Engineering and Soil Dynamics*. 1.
http://scholarsmine.mst.edu/icrageesd/02icrageesd/session01/1

This Article - Conference proceedings is brought to you for free and open access by Scholars' Mine. It has been accepted for inclusion in International Conferences on Recent Advances in Geotechnical Earthquake Engineering and Soil Dynamics by an authorized administrator of Scholars' Mine. This work is protected by U. S. Copyright Law. Unauthorized use including reproduction for redistribution requires the permission of the copyright holder. For more information, please contact scholarsmine@mst.edu.

Proceedings: Second International Conference on Recent Advances in Geotechnical Earthquake Engineering and Soil Dynamics, March 11-15, 1991, St. Louis, Missouri, Paper No. 1.24

A Cyclic Shear-Volume Coupling and Pore Pressure Model for Sand

Peter M. Byrne
Professor of Civil Engineering, University of British Columbia, Vancouver, B.C., Canada

SYNOPSIS: A two parameter incremental shear-volume coupling equation is presented for sand. The equation is based upon experimental data and gives predictions that are in excellent agreement with data over a range of relative densities and stress conditions. Empirical expressions for the two parameters based on incorporated in a simple shear pore pressure element model and the predictions of the model are compared with both saturated undrained cyclic strain and cyclic load tests. It is found that, provided a threshold strain is incorporated, the model predictions are in very good agreement with the laboratory data over a wide range of stress and density conditions. The element model is also calibrated against field experience during earthquakes, and predicts pore pressure rise and liquefaction behaviour in close agreement with current design practice. The model can easily be calibrated to represent any cyclic loading data and is appropriate for incorporation in "loose coupled" dynamic analyses procedures such as those employed by Finn and his colleagues.

INTRODUCTION

Cyclic shear loading can induce significant volumetric compression strains in unsaturated sands which can result in undesirable ground settlements and possible damage to structures. In saturated sands, such loading can induce pore pressure rise and liquefaction which may result in severe damage to structures. Cyclic loading may arise from a number of causes, including earthquakes, ice loading, blasting, machine vibration, wind and wave loading.

Experimental evidence indicates that volumetric compression strains are induced by cyclic shear strain due to a coupling between the shear and volumetric response of sand. These volumetric strains are plastic in nature rather than elastic as they are not recovered at the end of a loading cycle. A rigorous effective stress dynamic analysis of soil structures comprised of sandy material requires a stress-strain law that includes shear-volume coupling effects for repeated load cycles. Such a stress-strain law is very complex and will require many parameters to adequately model the observed laboratory and field behaviour under cyclic loading conditions.

A simple effective stress analysis approach was first proposed by Martin et al. (1975). The basis of the approach is an equation linking the increment of volumetric strain per cycle of load with the shear strain occurring during that particular cycle. For a drained condition, the increments can be simply added to give the accumulated volumetric strain with number of cycles as carried out by Finn and Byrne (1976).

For an undrained condition the increment of volumetric strain will lead to a rise in porewater pressure that can be computed by imposing volume constraints together with an elastic rebound modulus. Pore pressure computed in this way can be incorporated in a simple incremental elastic dynamic response analysis in which the tangent stiffness is modified with both the level of shear strain and the pore pressure rise. Since the pore pressures can only be computed after each cycle or 1/2 cycle of strain as the analysis proceeds, this procedure is referred to as loose-coupled. The first effective stress dynamic analyses by this procedure were presented by Finn, Byrne and Martin (1976). The procedure has since been extensively developed by Finn et al. (1986).

A key factor in the loose-coupled effective stress approach is the cyclic shear-volume coupling equation. Martin et al. proposed a 4 parameter equation based on laboratory data on a single sand at a single relative density. Finn and Byrne (1976) suggested an additional equation for predicting volume changes at other relative densities. A detailed examination of the Martin et al. equation shows that it is not generally stable. Herein, an alternative two parameter equation is proposed that gives excellent agreement with measurements over a range of relative densities. The parameters can easily be derived from cyclic loading tests, or can be estimated from relative density or penetration values based upon available data. The parameters can be used in analysis to predict expected plastic volume changes and settlements under dry or drained conditions and/or pore pressure rise and liquefaction of saturated sands in either an effective or total stress dynamic analysis.

CYCLIC SHEAR-VOLUME COUPLING EQUATION

Martin et al. (1975) proposed the following incremental shear-volume coupling equation for sand under simple shear loading:

$$\Delta\epsilon_v = C_1(\gamma - C_2\,\epsilon_v) + \frac{C_3\,(\epsilon_v)^2}{\gamma + C_4\,\epsilon_v} \qquad (1)$$

in which

$\Delta\epsilon_v$ = the increment of volumetric strain in percent per cycle of shear strain,

ϵ_v = the accumulated volumetric strain from previous cycles in per cent,

γ = the amplitude of shear strain in per cent for the cycle in question, and

C_1, C_2 C_3, C_4 = constants for the sand in question at the relative density under consideration.

The basic data used by Martin et al. to determine their equation is shown in Fig. 1 and comprises accumulated volumetric strain versus number of cycles from simple shear tests on crystal silica sand conducted at three different levels of shear strain and a relative density of 45%.

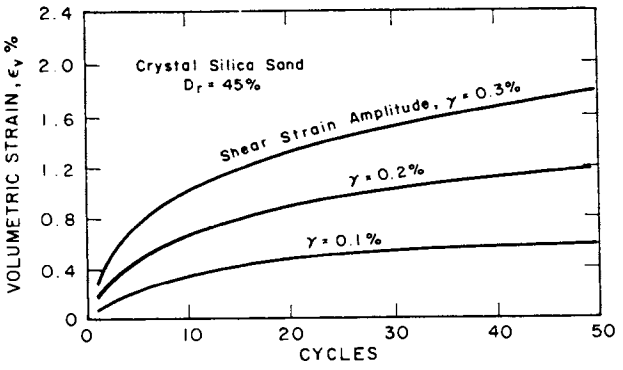

Fig. 1. Volumetric strains from constant amplitude cyclic simple tests. Test data from Martin et al. (1975).

It may be seen from Fig. 1 that the volumetric strain increases with the level of shear strain applied, and that for the same level of shear strain, the rate of accumulation of volumetric strain reduces with number of cycles. Martin et al. plotted this same data in an incremental form as shown in Fig. 2, and it indicates that the volumetric strain per cycle, $\Delta\epsilon_v$, depends upon the current level of applied strain as well as the accumulated volumetric strain, i.e., the accumulated volumetric strain is the hardener that controls the plastic volume change in the current cycle. Also, in this form it is not necessary that the shear strain be the same for every cycle in a loading sequence. However, from this figure, it is difficult to express the data in equation form.

An alternative form to plot the data of Fig. 1 is shown in Fig. 3 in which the volumetric

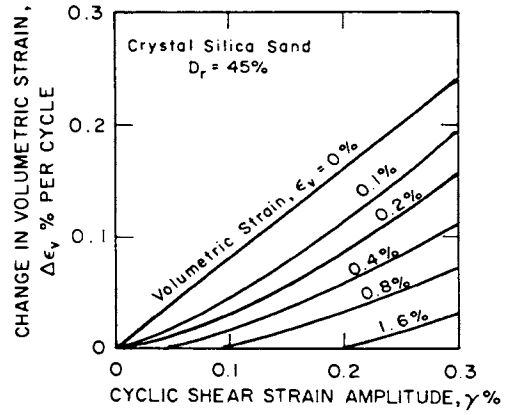

Fig. 2. Incremental volumetric strain curves from the data of Fig 1.

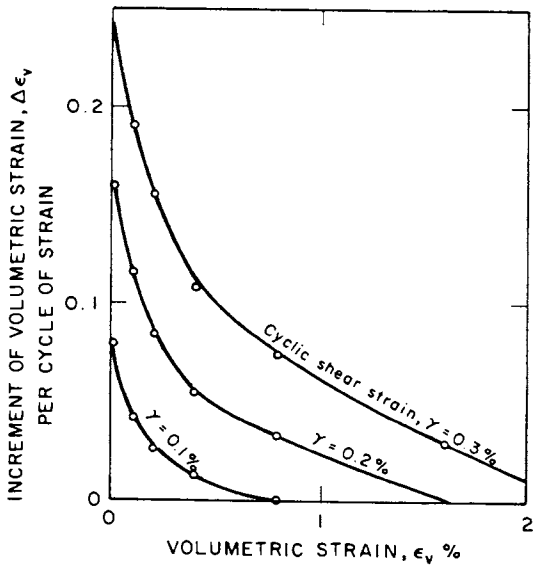

Fig. 3. Alternative volumetric strain curves from the data of Fig. 1.

strain per cycle, $\Delta\epsilon_v$, is plotted versus the accumulated volumetric strain, ϵ_v, for the three levels of shear strain. If the axes of Fig. 3 are divided by the shear strain, the three curves of Fig. 3 collapse to the single curve in the dimensionless plot shown in Fig. 4. This curve is well represented by

$$\frac{\Delta\epsilon_v}{\gamma} = C_1\ \mathrm{EXP}\left(-C_2\left(\frac{\epsilon_v}{\gamma}\right)\right) \qquad (2)$$

where C_1 = 0.8 and C_2 = 0.5 for the data shown.

The parameter C_1 controls the amount of volume change.

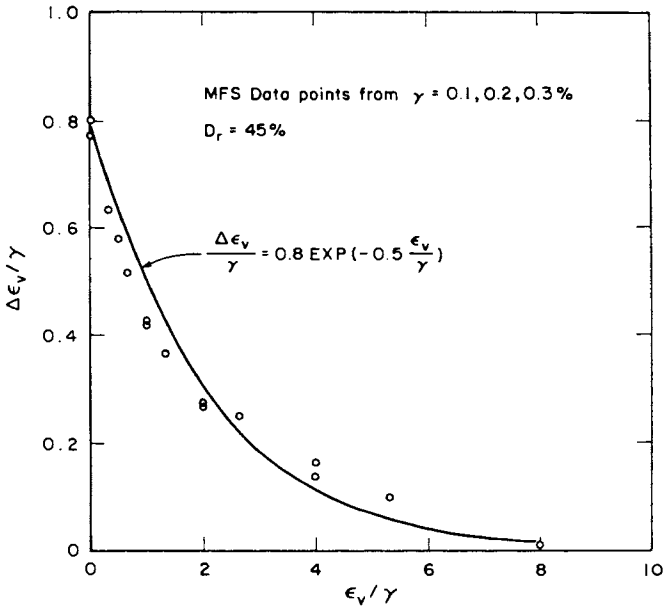

Fig. 4. Normalized incremental volumetric strains.

For the first cycle of loading $\epsilon_v = 0$ and hence

$$C_1 = \frac{(\Delta\epsilon_v)_{cycle\ 1}}{\gamma} \quad (3)$$

The data also shows that the accumulated volumetric strain at the end of 15 uniform cycles is about 5 times greater than for the 1st cycle, hence

$$C_1 = \frac{(\epsilon_v)_{15}}{5\,\gamma} \quad (4)$$

This equation may be preferable to equation (3) in many instances, because there is considerable data on $(\epsilon_v)_{15}$ as a function of relative density.

The parameter C_2 controls the shape of the accumulated volume change with number of cycles. The predicted shape is shown in Fig. 5 and is in good agreement with the Martin et al. data as well as the Tokimatsu and Seed (1987) data. The Tokimatsu and Seed data is for a range of relative densities, while the Martin et al. data is just for D_r = 45%.

Since the shape is the same for all densities the parameter C_2 is a constant fraction of C_1 for all relative densities and can be prescribed as:

$$C_2 = 0.4/C_1 \quad (5)$$

The fundamental incremental shear-volume coupling equation therefore involves only one constant, C_1, which depends on the density of the sand and can be simply assessed if the

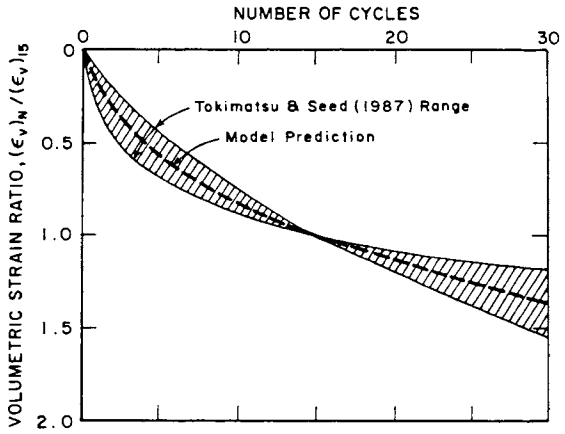

Fig. 5. Relationship between volumetric strain ratio and number of cycles for dry sands. Test data from Tokimatsu and Seed (1987).

accumulated volumetric strain at any specific number of cycles is known. However, it is suggested that the second constant C_2 be preserved as it gives greater flexibility in matching the data if a more complete history of accumulated volumetric strain is available.

Tokimatsu and Seed (1987) have presented accumulated volumetric strains data after 15 cycles for a range of cyclic shear strains and relative densities and these are shown in Fig. 6. The solid lines represent the

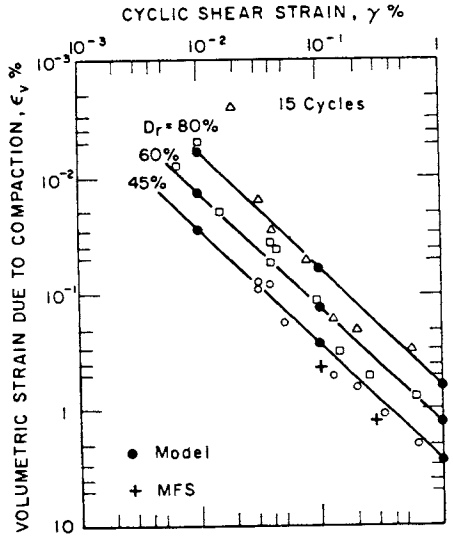

Fig. 6. Relationship between volumetric strain and shear strain for dry sands. Test data from Silver and Seed (1971).

Tokimatsu and Seed interpretation of the data, and based on their lines, and using Eqs. (4) and (5), the following values of C_1 and C_2 are computed:

Table 1. C_1 and C_2 from Relative Density

D_r	$(\epsilon_v^p)_{15}/\gamma$	C_1	C_2
45	2.8	0.56	0.71
60	1.2	0.24	1.66
80	0.65	0.13	3.08

The model predictions using these values of C_1 and C_2 are also shown in Fig. 6 and are seen to be in excellent agreement with the data. The Martin et al. data is also shown on this figure and denoted by MFS, and is seen to lie below the Tokimatsu and Seed data.

The C_1 value can be expressed in equation form as follows:

$$C_1 = 7600\ (D_r)^{-2.5} \tag{6}$$

in which D_r is in %, and

$$C_2 = 0.4/C_1 \tag{7}$$

Tokimatsu and Seed also show values of accumulated volumetric strains after 15 cycles as a function of normalized standard penetration test values $(N_1)_{60}$. Their data is not shown as it just involves a conversion from D_r to $(N_1)_{60}$.

The conversion between relative density and $(N_1)_{60}$ used by Tokimatsu and Seed can be approximated in the range $30 < D_r < 90$ by:

$$D_r = 15(N_1)_{60}^{1/2} \tag{8}$$

Based on their data and using Eqs. (4) and (6), the values of C_1 and C_2 are as follows:

Table 2. C_1 and C_2 from SPT N Values

$(N_1)_{60}$	$(\epsilon_v^p)_{15}/\gamma$	C_1	C_2
5	5	1	0.4
10	2.5	0.5	0.8
20	1.0	0.2	2.0
30	0.6	0.12	3.33
40	0.3	0.06	6.66

The C_1 and C_2 values can be expressed in equation form as follows:

$$C_1 = 8.7\ (N_1)_{60}^{-1.25} \tag{9}$$

$$C_2 = 0.4/C_1 \tag{10}$$

The volumetric strain equation can be incorporated in a dynamic analysis to compute the volumetric strains arising from any one-dimensional series of strain pulses at any depth in a sand stratum. Integration of such strains will give the settlement at any point within the stratum.

For a random pattern of strain cycles it is appropriate to modify the basic equation to compute the volumetric strains per 1/2 cycle as follows:

$$(\Delta\epsilon_v)_{1/2\ cycle} = 0.5\ \gamma\ C_1\ EXP(-C_2\frac{\epsilon_v}{\gamma}) \tag{11}$$

The volumetric strains can also be used to compute pore pressure rise and liquefaction and this is discussed in the next section.

VOLUMETRIC STRAIN AND PORE PRESSURE RISE

If the pores of the sand are saturated with water and if the water has not sufficient time to drain during the cycles of loading, the pore pressure will rise and liquefaction may occur. The pore pressure rise for saturated undrained conditions can be computed from volume compatibility as follows:

$$\Delta\epsilon_v = \Delta\epsilon_v^e + \Delta\epsilon_v^p \tag{12}$$

in which

$\Delta\epsilon_v$ = the total incremental change in volumetric strain per 1/2 cycle

$\Delta\epsilon_v^e$ = the elastic incremental change in volumetric strain per 1/2 cycle

$\Delta\epsilon_v^p$ = the plastic incremental volumetric strain per 1/2 cycle

now for simple shear conditions

$$\Delta\epsilon_v^e = \frac{\Delta\sigma_v'}{M} \tag{13}$$

where

$\Delta\sigma_v'$ = the change in vertical effective stress per 1/2 cycle

M = the constrained rebound effective stress tangent modulus of the sand skeleton

The volumetric strains referred to in the previous section and in particular Eq. (11) are not recoverable and are therefore plastic strains, and in the discussion to follow will be given the superscript p.

For saturated undrained conditions $\Delta\epsilon_v \approx 0$, and hence from Eqs. (12) and (13),

$$\Delta\sigma_v' = -M\ \Delta\epsilon_v^p \tag{14}$$

If there is no change in total stress then $\Delta\sigma_v = 0$, and the change in porewater pressure $\Delta u_v = -\Delta\sigma$, hence

$$\Delta u = M\ \Delta\epsilon_v^p \qquad (15)$$

Knowing $\Delta\epsilon_v^p$ from Eq. (11) for any known half cycle of strain, the pore pressure rise per half cycle can be computed from Eq. (15). The pore pressure generated, u_g, by any specified pattern of strain cycles can be computed by simply summing the pore pressure increments, i.e., $u_g = \Sigma\Delta u$.

The appropriate rebound effective stress constrained tangent modulus, M appears to depend only upon the level of effective stress and not the relative density, and can be prescribed as follows:

$$M = K_m P_a \left(\frac{\sigma'_v}{P_a}\right)^m \qquad (16)$$

Values of $K_m \approx 1600$ and $m = 0.5$ give moduli that are in good agreement with values reported by Martin et al. (1975) as well as results of liquefaction tests.

CYCLIC STRAIN CONTROLLED RESPONSE

A pore pressure model for predicting simple shear response of a sand element under prescribed cycles of shear strain can be developed from the equations presented in the previous sections and these have been incorporated in the computer code SSLIQ (Byrne, 1990). The purpose here is to check this model against laboratory data.

Pore pressure rise from cyclic strain controlled tests are shown in Fig. 7 and indicate that there is a threshold shear strain below which plastic volumetric strains and pore pressure rise will not occur in undrained tests. These tests involve a very large number of cycles. It was found that the model based on Eq. 11 overpredicted the volumetric strains and pore pressures. A correction to the shear strain to account for threshold strain is necessary to obtain reasonable agreement with the data.

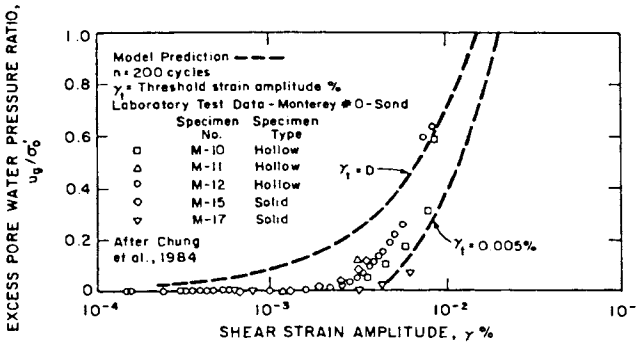

Fig. 7. Excess porewater pressure build-up versus shear strain amplitude, resonant column tests.

The threshold strain effect is accounted for by specifying an effective or plastic shear strain, γ^*, to be used in Eq. (11) as follows:

$$\gamma^* = \gamma - \gamma_t \qquad (17)$$

in which

γ_t = the threshold strain

Model predictions with $\gamma_t = 0$ and 0.005% are shown in Fig. 7. $\gamma_t = 0$ clearly overpredicts the pore pressure response while $\gamma_t = 0.005\%$ gives a lower bound to the response. $\gamma_t = .002\%$ gave a best fit to the data but is not shown on the figure for clarity.

Strain controlled cyclic triaxial tests reported by NRC (1985) and attributed to Dobry are shown in Fig. 8 and indicate that little pore pressure is generated for 10 cycles of strain if the cyclic strain is less than 0.01%. $\gamma_t = .005\%$ gives an upper bound to this data. Based upon the data of these two figures a compromise $\gamma_t = 0.005\%$ was selected for calibration with the results of load controlled tests.

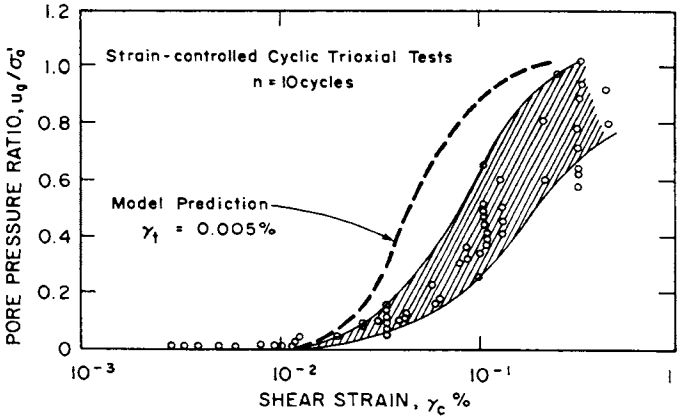

Fig. 8. Excess porewater pressure build-up. Test data from NRC (1985).

CYCLIC LOAD CONTROLLED RESPONSE

In predicting the cyclic load controlled undrained response of saturated sand using the proposed model, it is necessary to introduce a shear-stress strain law in order to compute shear strains from the applied shear stresses.

Shear Stress-Strain Law

Numerous researchers (Seed & Idriss (1970); Hardin & Drnevich (1972); Tokimatsu & Seed (1987)), have proposed shear stress-strain relations for sand. The relations are nonlinear but are generally expressed using a strain compatible secant modulus that is usually specified in terms of a maximum shear modulus, G_{max} and a modulus reduction factor that depends upon the level of shear stress

or strain. Based on Seed and Idriss (1970), the maximum shear modulus, G_{max} which occurs at shear strain values of less than 10^{-4}% can be expressed as:

$$G_{max} = 21.7\ (K_2)_{max}\ P_a \left(\frac{\sigma'_m}{P_a}\right)^{0.5} \qquad (18)$$

which

$(K_2)_{max}$ = a modulus parameter that depends on the density or $(N_1)_{60}$ value of the sand

P_a = atmospheric pressure in the units used

and

σ'_m = the mean normal effective stress

Seed and Idriss (1970) data on $(k_2)_{max}$ indicates that it can be expressed as a function of D_r by the following equation:

$$(k_2)_{max} = 3.5\ (D_r)^{2/3} \qquad (19)$$

in which D_r is in %.

In terms of $(N_1)_{60}$, Seed et al. (1986) suggest that,

$$(K_2)_{max} = 20(N_1)_{60}^{1/3} \qquad (20)$$

Equations (18), (19), and/or (20) allow G_{max} to be computed when the effective stresses and $(N_1)_{60}$ or relative density are known.

Hardin and Drnevich (1972), Seed et al. (1986) and Tokimatsu and Seed (1987) propose modulus reduction curves that allow the appropriate strain compatible secant modulus to be computed. The Hardin and Drnevich approach is used here as it gives results similar to Seed et al. and is readily expressed in mathematical form as follows:

$$G = G_{max} = \left(\frac{1}{1+\gamma_h}\right) \qquad (21)$$

in which γ_h = hyperbolic strain. The details involved in computing γ_h are given in the Appendix.

Liquefaction Resistance

The shear stress-strain equations were incorporated in the SSLIQ program. This allows the shear strain to be computed for the prescribed shear stress, and account is taken of the rising pore pressure and its effect on the shear modulus.

The predicted liquefaction resistance curves are compared with laboratory measured values for three different relative densities in Fig. 9. It may be seen that both the characteristic shape of the predicted curves as well as the actual stress ratio values are in good agreement with the measurements over the range of relative densities.

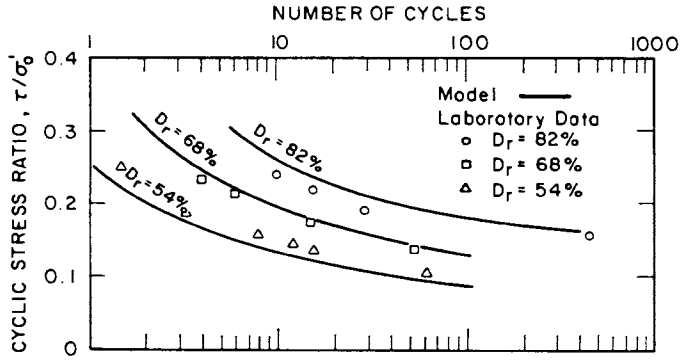

Fig. 9. Cyclic stress ratio versus number of cyclic to initial liquefaction. Test data from shaking table tests, De Alba et al. (1976).

The characteristic shape of the liquefaction resistance curves can be better examined in terms of a dimensionless stress ratio τ_N/τ_{15} versus the number of cycles to liquefaction and this is shown in Fig. 10. Both the laboratory data and the model predictions are for a range of relative densities and normal stresses. It was found that the characteristical shape was strongly dependent on the threshold strain value assumed and this is shown in the figure. For a threshold strain value of zero, as was initially considered, a poor fit was obtained (not shown). The best fit was obtained using a threshold strain γ_t = 0.01%. An adequate fit is obtained with γ_t = 0.005%, and this value is used in all other model predictions.

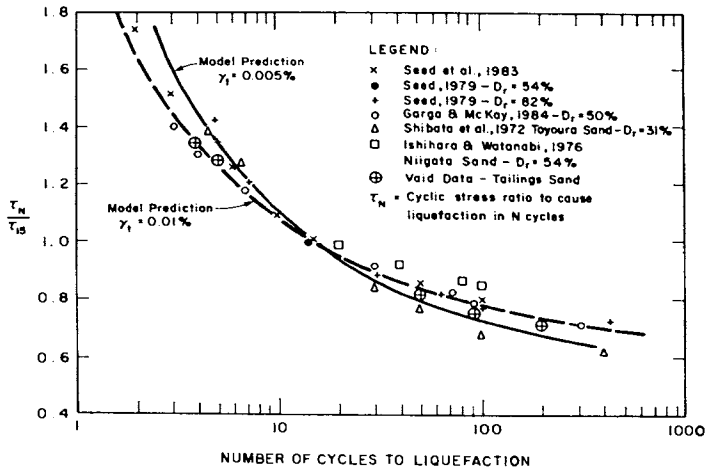

Fig. 10. Relationship between shear stress level and the number of cycles to cause initial liquefaction.

Liquefaction resistance curves presented by Seed et al. (1985) and based on field observations during past earthquakes are presented in Fig. 11. These curves presently represent the state of the practice and are based on stress ratios computed from the earthquake,

normalized standard penetration resistance values $(N_1)_{60}$ at the sites in question, and field evidence of liquefaction. The chart lines are considered to represent the field resistance for M7.5 earthquakes causing 15 load cycles.

The model prediction for initial liquefaction, $u_g/\sigma_o' = 1$ in 15 cycles, is shown as the dashed line in Fig. 11. It is generally in

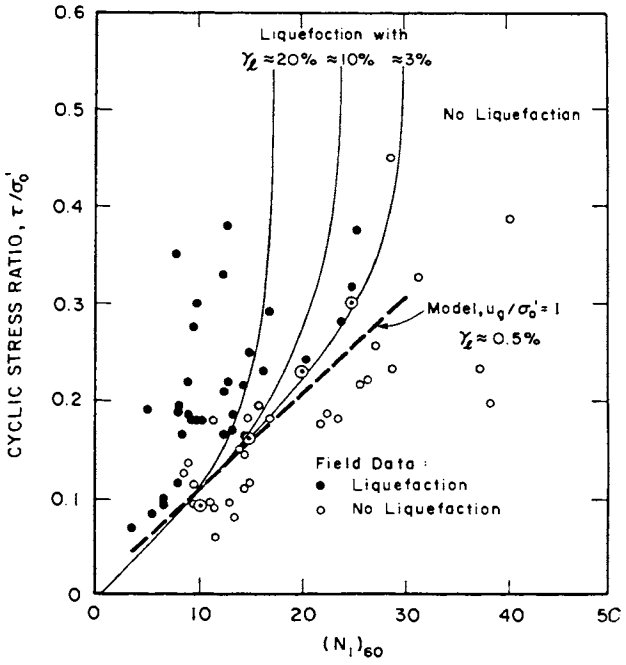

Fig. 11. Relationship between cyclic stress ratio, $(N_1)_{60}$ value and liquefaction, M=7.5. Test data from Seed et al. (1984).

close agreement with the field data except at the higher $(N_1)_{60}$ values, where the model predictions lie below the Seed line. The lowest Seed line is for a cyclic strain amplitude of 3%. Initial liquefaction occurs at strains of less than 0.5%, and for the denser material with the high $(N_1)_{60}$ value, additional cycles would be required to induce 3% strains and this may account for the divergence in the predicted and observed response shown. At the lower densities, large strains occur as soon as the initial liquefaction condition is reached, so that the curves for all strains converge as shown at lower $(N_1)_{60}$ values.

The characteristic shape of the pore pressure rise curve with number of constant amplitude load cycles is examined in Fig. 12. The number of cycles is expressed in dimensionless form as the ratio of the current cycle number, n, to the number of cycles to cause initial liquefaction, n_L. It may be seen that the model prediction lies within the measured data.

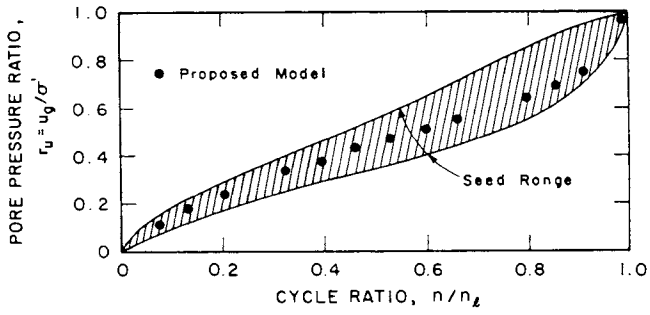

Fig. 12. Rate of pore pressure build-up in cyclic simple shear. Test data from Seed et al. (1976).

The generated pore pressure ratio as a function of factor of safety against tiggering liquefaction is shown in Fig. 13. The factor of safety is defined as the ratio of the stress ratio to cause liquefaction to the applied stress ratio, and the pore pressures are examined at $n = n_L$. Also shown on the figures is laboratory data on a range of sand and gravels. The model results follow the trend of the measurements and plot near the upper bound for sands.

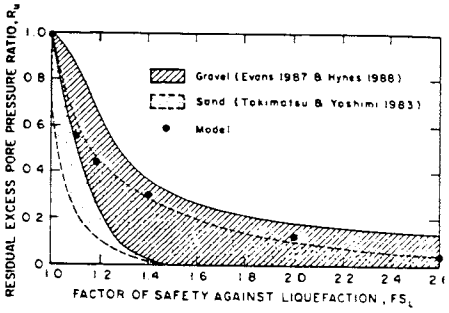

Fig. 13. Excess Porewater Pressure and Factor of Safety Against Liquefaction. Test data from Marcuson et al. (1990).

SUMMARY

A simple 2 parameter incremental shear-volume coupling equation has been presented for sand. The equation is based upon laboratory data and gives predictions that are in very good agreement with laboratory data over a range of relative densities. The model parameters can be obtained from laboratory tests or they may be estimated from existing data if the relative density or $(N_1)_{60}$ value of the sand is known.

The shear-volume coupling equation is incorporated in a cyclic simple shear pore pressure element model which includes an elastic rebound modulus equation that allows the excess pore pressures to be computed for any prescribed cyclic shear strain history. A comparison with laboratory cyclic strain test data indicates that there is a threshold

shear strain, γ_t, whose value is in the range 2.10^{-3} to 10^{-2}% below which plastic volumetric strain and pore pressure rise does not occur. The existing data suggests that γ_t = 0.005% is appropriate.

The model is extended to cyclic loading tests by the introduction of a shear stress-strain law in which the shear modulus is modified for both the current strain and excess pore-water pressure. This allows the appropriate shear strain to be computed for the current cycle.

The model predictions are compared with laboratory cyclic load tests and field experience during earthquakes, and found to be generally in excellent agreement both in terms of trends and in terms of specific values.

The model parameters are easily obtained from specific test data using the interactive computer code SSLIQ. Parameters that will match existing design curves based on $(N_1)_{60}$ values are built into SSLIQ. These parameters may then be incorporated in dynamic analysis programs such as 1-DLIQ (Byrne and Yan, 1990), based on Finn, Byrne and Martin (1976), or they could be incorporated in a modified version of TARA-3 (Finn et al., 1986).

ACKNOWLEDGEMENT

The author is grateful to Mr. Li Yan for his critical review of the paper and to Mrs. K. Lamb for typing and presentation. The author also acknowledges the financial support of NSERC Canada.

REFERENCES

Byrne, P.M., "SSLIQ: A Computer Code for Predicting the Simple Shear Response of a Sand Element to Cyclic Loading", Soil Mechanics Series No. 145, Dept. of Civil Engineering, University of British Columbia, August 1990.

Byrne, P.M. and Yan, L., "ID-LIQ: A Computer Code for Predicting the Effective Stress 1-Dimensional Response of Soil Layers to Seismic Loading", Soil Mechanics Series No. 146, Dept. of Civil Engineering, University of British Columbia, September 1990.

Chung, R.M., Yokel, F.Y. and Drnevich, V.P., "Evaluation of Dynamic Properties of Sands by Resonant Column Testing", Geotechnical Testing Journal, ASTM, Vol. 7, No. 2, June 1984, pp. 60-69.

De Alba, P., Seed, H.B. and Chan, C.K., "Sand Liquefaction in Large-Scale Simple Shear Tests", Journal of the Geotechnical Engineering Division, ASCE, Vol. 102, No. GT9, September 1976, pp. 909-927.

Finn, W.D. Liam and Byrne, P.M., "Estimating Settlements in Dry Sands During Earthquakes", Canadian Geotechnical Journal, 1976, Vol. 13, No. 4.

Finn, W.D. Liam, Byrne, P.M. and Martin, G.R., "Seismic Response and Liquefaction of Sands", Journal of the Geotechnical Eng. Division, ASCE, No. GT8, August 1976.

Finn, W.D. Liam, Yogendrakumar, M., Yoshida, N. and Yoshida, H., "TARA-3: A Program to Compute the Response of 2-D Embankments and Soil-Structure Interaction Systems to Seismic Loadings", Dept. of Civil Engineering, University of British Columbia, Vancouver, B.C., Canada, 1986.

Hardin, B.O. and Drnevich, V.P., "Shear Modulus and Damping Curves in Soils: Design Equations and Curves", Journal of the Soil Mech. and Foundations Division, ASCE, 1972, No. SM7.

Marcuson III, W.E., Hynes, M.E. and Franklin, A.G., "Evaluation and Use of Residual Strength in Seismic Safety Analysis of Dams", Earthquake Spectra, Vol. 6, No. 3, August 1990.

Martin, G.R., Finn, W.D. Liam and Seed, H.B., "Fundamentals of Liquefaction Under Cyclic Loading", Journal of the Geotechnical Eng. Division, ASCE, May 1975, Vol. 101, No. GT5.

National Research Council, Committee on Earthquake Engineering, Commission on Engineering and Technical Systems, "Liquefaction of Soils During Earthquakes", National Academy Press, Washington, D.C., 1985.

Seed, H.B. and Idriss, I.M., "Soil Moduli and Damping Factors for Dynamic Response Analysis", Rpt. No. UCB/EERC-70/10, University of California, Berkeley, 1970.

Seed, H.B., Martin, P.P. and Lysmer, J., "Pore-Water Pressure Changes During Soil Liquefaction", Journal of the Geotechnical Engineering Division, ASCE, Vol. 102, No. GT4, April 1976, pp. 323-346.

Seed, H.B., Wong, R.T., Idriss, I.M. and Tokimatsu, K., "Moduli and Damping Factors for Dynamic Analyses of Cohesionless Soils", Journal of Geotechnical Eng., November 1986, Vol. 112, No. 11.

Seed, H.B., Tokimatsu, K., Harder, L.F. and Chung, R., "Influence of SPT Procedures in Soil Liquefaction Resistance Evaluations", Journal of Geotechnical Eng., ASCE, 1985, Vol. 111, No. 12.

Tokimatsu, K. and Seed, H.B., "Evaluation of Settlements in Sands Due to Earthquake Shaking", Journal of Geotechnical Eng., ASCE, 1987, Vol. 113, No. 8, pp. 861-878.

APPENDIX

Shear Modulus

The appropriate secant shear modulus was specified by Equation (21) in the text, namely:

$$G = G_{max} \left(\frac{1}{1 + \gamma_h}\right) \quad (A1)$$

where

$$\gamma_h = \frac{\gamma}{\gamma_{ref}} [1 + a \, EXP(-b \frac{\gamma}{\gamma_{ref}})] \quad (A2)$$

$$a = -0.2 \log N_{cyc} \quad (A3)$$

$$b = 0.16$$

$$\gamma_{ref} = \tau_{max}/G_{max} \quad (A4)$$

and

$$\tau_{max} = [(\frac{1+K_o}{2} \sigma'_v \sin\phi)^2 - (\frac{1-K_o}{2} \sigma'_v)^2]^{1/2} \quad (A5)$$

where

K_o = the at-rest pressure coefficient

ϕ' = the effective friction angle of the sand given by

$$\phi' = \phi'_i - \Delta\phi' \log(\sigma'_m/p_a) \quad (A6)$$

$$\phi'_i = 32° + (N_1)_{60}/3 \quad (A7)$$

and

$$\Delta\phi' = 0.18 \, (N_1)_{60} \quad (A8)$$

σ'_v = the vertical effective stress

If a and b are taken to be zero, then

$$G = G_{max} \, (1 - \tau_{cyc}/\tau_{max}) \quad (A9)$$

The modulus reduction curves G/G_{max} defined by either Eq. (A1) or (A9) essentially fall within the modulus reduction band suggested by Seed et al. (1986). Equation (A1) was used in all predictions.